

Large-scale Rossby Normal Modes During some Recent Northern Hemisphere Winters

F. Sassi

Naval Research Laboratory - Space Science Division

R.R. Garcia

National Center for Atmospheric Research

K. W. Hoppel

Naval Research Laboratory - Remote Sensing Division

Corresponding author:

Dr. F. Sassi

Naval Research Laboratory

Space Science Division

4555 Overlook Ave SW

Washington DC - 20375

Report Documentation Page			Form Approved OMB No. 0704-0188		
Public reporting burden for the collection of information is estimated to average 1 hour per response, including the time for reviewing instructions, searching existing data sources, gathering and maintaining the data needed, and completing and reviewing the collection of information. Send comments regarding this burden estimate or any other aspect of this collection of information, including suggestions for reducing this burden, to Washington Headquarters Services, Directorate for Information Operations and Reports, 1215 Jefferson Davis Highway, Suite 1204, Arlington VA 22202-4302. Respondents should be aware that notwithstanding any other provision of law, no person shall be subject to a penalty for failing to comply with a collection of information if it does not display a currently valid OMB control number.					
1. REPORT DATE 2011		2. REPORT TYPE		3. DATES COVERED 00-00-2011 to 00-00-2011	
4. TITLE AND SUBTITLE Large-scale Rossby Normal Modes During some Recent Northern Hemisphere Winters				5a. CONTRACT NUMBER	
				5b. GRANT NUMBER	
				5c. PROGRAM ELEMENT NUMBER	
6. AUTHOR(S)				5d. PROJECT NUMBER	
				5e. TASK NUMBER	
				5f. WORK UNIT NUMBER	
7. PERFORMING ORGANIZATION NAME(S) AND ADDRESS(ES) Naval Research Laboratory, Space Science Division, 4555 Overlook Ave SW, Washington, DC, 20375				8. PERFORMING ORGANIZATION REPORT NUMBER	
9. SPONSORING/MONITORING AGENCY NAME(S) AND ADDRESS(ES)				10. SPONSOR/MONITOR'S ACRONYM(S)	
				11. SPONSOR/MONITOR'S REPORT NUMBER(S)	
12. DISTRIBUTION/AVAILABILITY STATEMENT Approved for public release; distribution unlimited					
13. SUPPLEMENTARY NOTES J. Atmos. Sci., submitted					
14. ABSTRACT Wavenumber-1 Rossby normal modes are studied for the Northern Hemisphere winters of 2005, 2006, 2008 and 2009 using global observational meteorological analyses spanning the 0-100 km altitude range. Spectral analysis of geopotential height fields shows pronounced peaks at westward propagating zonal wave number 1 near the theoretical locations of the free Rossby waves at 25 days, 16 days, 10 days and 5 days that, in some cases, have amplitudes significantly larger than the estimated background spectrum. A coherence analysis is used to extract the amplitude and phase of the waves, and to isolate those regions of the latitude/altitude plane where the signals are statistically significant. Although the spectral location, temporal evolution and vertical structure of several of these waves are suggestive of the presence of Rossby normal modes, this study shows that in the real atmosphere the waves only occasionally have the global properties of classical normal modes. Moreover, we find no evidence that the amplitudes of these modes are enhanced during stratospheric sudden warmings.					
15. SUBJECT TERMS					
16. SECURITY CLASSIFICATION OF:			17. LIMITATION OF ABSTRACT Same as Report (SAR)	18. NUMBER OF PAGES 51	19a. NAME OF RESPONSIBLE PERSON
a. REPORT unclassified	b. ABSTRACT unclassified	c. THIS PAGE unclassified			

Abstract

Wavenumber-1 Rossby normal modes are studied for the Northern Hemisphere winters of 2005, 2006, 2008 and 2009 using global observational meteorological analyses spanning the 0-100 km altitude range. Spectral analysis of geopotential height fields shows pronounced peaks at westward propagating zonal wave number 1 near the theoretical locations of the free Rossby waves at 25 days, 16 days, 10 days and 5 days that, in some cases, have amplitudes significantly larger than the estimated background spectrum. A coherence analysis is used to extract the amplitude and phase of the waves, and to isolate those regions of the latitude/altitude plane where the signals are statistically significant. Although the spectral location, temporal evolution and vertical structure of several of these waves are suggestive of the presence of Rossby normal modes, this study shows that in the real atmosphere the waves only occasionally have the global properties of classical normal modes. Moreover, we find no evidence that the amplitudes of these modes are enhanced during stratospheric sudden warmings.

1. Introduction

The existence of large-scale free Rossby waves in the atmosphere has been known for many decades (e.g., Eliassen and Machenauer, 1965, 1969), and the theory dates back to the 19th century (see Madden, 2007, for a historical perspective). Substantial theoretical progress was made with the calculations of Longuet-Higgins (1968), who described the solutions of Laplace's tidal equation in an isothermal atmosphere using different equivalent depths, including structures corresponding to normal, or "free", modes. The behavior of normal modes in the presence of a realistic background atmosphere was calculated numerically by Salby (1981b) using prescribed climatological background winds and temperatures typical of solstice and equinox. Salby (1981a) also showed that inhomogeneities in the background atmosphere can lead to spectral broadening, Doppler shifting and distortion of the energy associated with the westward propagating normal modes. A recent review of atmospheric normal modes, their spatial structure and temporal behavior is provided by Madden (2007).

The existence of some of these modes in the real atmosphere has been documented by several authors. Some of the free modes that are most frequently identified in the atmosphere at zonal wavenumber 1 have characteristic periods of 25, 16, 10 and 5 days. Their theoretical horizontal structures are shown in Fig. 1 in terms of the normalized amplitude of the geopotential: the 25-day wave has the structure of the Rossby (1,4) normal mode which is anti-symmetric about the equator with three nodes in the meridional direction; the 16-day wave has the structure of the symmetric Rossby (1,3) mode and two nodes; the 10-day wave corresponds to the structure of the anti-symmetric (1,2) Rossby mode with one node at the equator; and, the 5-day wave to the Rossby (1,1) mode has no nodal points in the meridional direction.

Evidence of the 25-day mode is provided by Madden (2007) and references therein. The 16-day wave has been observed ubiquitously in the troposphere (Madden, 1978) and in the middle atmosphere during winter (Forbes et al., 1995), as well as at the summer mesopause (Williams and Avery, 1992) and in the lower thermosphere (Namboothiri et al., 2002; Day and Mitchell, 2010). Espy et al. (1997) suggested that the presence of the 16-day wave at high latitudes of the summer mesopause is related to a favorable wind configuration in the tropical upper stratosphere. In some years, the 16-day mode has also been linked to an amplification of wave activity during a stratospheric warming (Smith, 1985), while at other times the relation to stratospheric warmings is not existent (Lou et al., 2000). Hirooka and Hirota (1985) document the intermittent synoptic structure of the 10-day and 16-day modes and their relation to the varying background atmospheric conditions. A 5-day oscillation has been identified in radar observations of the mesosphere and the lower thermosphere by Day and Mitchell (2010), and in satellite data by Wu et al. (1994). There is also observational evidence of a 5-day oscillation in global surface pressure (Madden and Julian, 1972). The 5-day wave has been investigated numerically by Salby (1981b) and Meyer and Forbes (1997). Free modes at higher zonal wave numbers were modeled by Salby (1981b) but they are difficult to identify in the atmosphere because of their small amplitude and their susceptibility to variations in the background winds.

A complication arising in real data is that no wave mode in the atmosphere is expected to appear as a pure normal (free) mode; rather, in some instances, waves are observed to exhibit behavior that resembles the normal modes. This occurs because variability of the background atmosphere and the presence of dissipation represent important departures from the conditions

assumed to derive the theoretical description of normal modes. Nevertheless, the occurrence of normal modes has been linked to weather patterns and precipitation events (Madden, 2007).

As noted above, Salby (1981b) discussed the effect of realistic background conditions on the behavior of the free modes using mean climatological winds in his numerical calculations. Salby's results raise interesting questions about the behavior of the normal modes during disturbed conditions in the middle atmosphere, such as those occurring during stratospheric sudden warmings (SSW). During SSW, the stratospheric polar vortex reverses from its climatological eastward flow to a westward flow. As the temperature is in approximate geostrophic balance with the zonal winds at middle and high latitudes, substantial temperature changes occur both in the stratosphere and in the mesosphere. These large perturbations to the background atmosphere may affect, not only the propagation through changes of the refractive index, but also the excitation of free modes. In fact, Hirooka and Hirota (1985) suggested that normal modes might be amplified during a sudden stratospheric warming (SSW), possible observational evidence for which was reported during SSWs by Dowdy et al. (2004), Espy et al. (2005) and Pancheva et al. (2008).

In this study, non-stationary, westward propagating atmospheric variability is examined during four recent northern hemisphere (NH) winters using global meteorological analyses that extend from ~0-92 km altitude. Prominent zonal wavenumber 1 (wave-1) modes at periods that correspond closely to the theoretical normal modes are identified, and their structure is examined for similarity with the theoretical free modes. The goal of this study is to document their structure during quiet, moderately disturbed and greatly disturbed northern hemisphere winters. A unique aspect of this study is the use of data assimilation products that extend to the

mesosphere and lower thermosphere (MLT: ~ 92 km) that offer for the first time the possibility to study transient behavior in a deep atmospheric column. The forecast-assimilation system and data assimilation products are described in Section 2. A description of the time mean and transient behavior of the background atmosphere during the northern hemisphere winters of 2005, 2006, 2008 and 2009 is given in Section 3. Spectral analyses of the filtered data products are shown in Section 4. The relation with SSW is discussed in Section 5. Conclusions are given in Section 6.

2. Data products and methodology

The observations-based products that form the basis of this study are 6 hourly global meteorological analyses from ~ 0 -95 km¹ altitude issued by an Advanced Level Physics High-Altitude (ALPHA) prototype of the Navy Operational Global Atmospheric Prediction System (NOGAPS). NOGAPS is the Department of Defense's operational global numerical weather prediction (NWP) system (Hogan and Rosmond 1991). NOGAPS-ALPHA is a high-altitude research prototype of that system that extends the vertical range and capabilities of both the forecast model and data assimilation system (DAS) components, thereby enabling the system to operate up to much higher altitudes (~ 95 km).

High-altitude global analyses were generated using the production NOGAPS-ALPHA configuration described in sections 2 and 3 of Eckermann et al. (2009), to which the interested reader is referred for full details. Briefly, the high-altitude forecast model component operates at horizontal resolution of T79 with 68 vertical levels from ~ 0 -95 km altitude, providing 0-9 hour

¹ This elevation and all others quoted in the following are log-pressure altitudes, using a scale height of 7 km.

forecast backgrounds to the Naval Research Laboratory (NRL) three-dimensional variational (3DVAR) DAS (NAVDAS: Daley and Barker 2001), which combines those forecast backgrounds with global observations to issue a global analysis field every 6 hours. In addition to the archived suite of satellite and suborbital observations from operational meteorological sensors that the standard NOGAPS assimilates, which extend from ~0-40 km altitude (see Baker et al. 2007), these production NOGAPS-ALPHA runs also assimilate version 2.2 limb retrievals of temperature, water vapor and ozone from the Microwave Limb Sounder (MLS) on NASA's Aura satellite and version 1.07 limb retrievals of temperature from the Sounding of the Atmosphere using Broadband Emission Radiometry (SABER) instrument on NASA's TIMED satellite. The MLS and SABER temperature observations are assimilated over the 32-0.002 hPa (~25-95 km altitude) range. Final analysis products are issued every 6 hours on a uniform $1^\circ \times 1^\circ$ global grid at a series of 60 reference pressure levels from the ground to ~100 km, distributed every ~2 km in the vertical throughout the middle atmosphere. These gridded analyses form the basis for the present study.

Several previous studies have confirmed that the zonal-mean state and planetary wave structures are captured accurately in these NOGAPS-ALPHA analyses at all altitudes, including the newly analyzed upper range of altitudes from ~50-90 km (Eckermann et al. 2009; Stevens et al. 2010; McCormack et al. 2010; Coy et al. 2011). Of particular relevance for the present study are the quasi-5 day Rossby (1,1) normal mode structures studied and validated by Eckermann et al. (2009) and Nielsen et al. (2010). Nielsen et al. (2010) showed how the temperature structure of the 5-day wave in the NOGAPS-ALPHA analyses during August 2007 was entirely consistent with independent observations of 5-day wave-1 modulation of polar mesospheric cloud (PMC)

brightness from NASA's Aeronomy of Ice in the Mesosphere (AIM) satellite. Given the demonstrated ability of the current NOGAPS-ALPHA configuration to capture the dominant planetary-scale motions of the atmosphere over the altitude range 0-95 km, we use these global analysis products to conduct a thorough investigation of Rossby normal modes over the entire range of analyzed altitudes for some northern hemisphere winter periods.

The first period (hereafter, winter of 2005) starts on November 20, 2004 and ends on March 30, 2005, for a total of 131 days. The second period (hereafter, winter of 2006) starts on December 20, 2005 and ends on March 20 2006, for a total of 90 days. The third period (hereafter, winter of 2008) starts on November 1, 2007 and ends on March 31, 2008, for a total of 152 days. The fourth and final period (hereafter, winter of 2009) begins on November 1, 2008, ending on April 30, 2009, and includes 181 days. The analyzed periods are also listed in Table 1.

We begin by computing daily averages to remove tides and other diurnal signals from the analyses. These diurnally-averaged analyses are next fitted globally using the first six Legendre polynomials, which provide sufficient meridional structure (with up to five meridional nodes) to resolve the structure of the gravest (wave-1) Rossby modes considered here while at the same time removing small-scale structures that could contaminate the analysis. Wave-1 is extracted using a Fast Fourier transform (FFT), and data from each period are spectrally analyzed after tapering the first and last 10% of the time series using a cosine function. The spectrum is obtained from the FFT of geopotential heights after the application of 5-point averaging in frequency.

In order to determine the statistical significance of the spectra, we compare the spectrum of the data to the spectrum of an autoregressive process of first order (AR1: Wilks, 2006); both the lag-1 auto-correlation and the white noise variance are determined by fitting the data spectrum to the theoretical spectrum of the AR1 process. The variance of the AR1 spectrum is then compared to the variance of the data spectrum; the latter is deemed statistically significant at any given frequency only when it exceeds the corresponding AR1 variance by a factor that is proportional to a critical value of χ^2 . Details of this calculation can be found in Wilks (2006) and are summarized in the Appendix. The Hayashi (1971) technique is used to calculate the amplitude and phase of the band-passed modes. Following Hayashi, a quadrature spectrum and a co-spectrum are calculated, using the spectral coefficients over a specified band, and a coherence squared analysis is used to evaluate the robustness of the wave structures, by focusing on the results where the coherence-squared exceeds 0.90.

3. Climatology of the four northern hemisphere winters

In this Section, a brief climatology of the four northern hemisphere winters is presented. As indicated in the previous Section, the NOGAPS-ALPHA data products have been extensively validated (Hoppel et al., 2008; Eckermann et al. 2009). Moreover, various aspects of the wintertime meteorology have been documented: the tropospheric pre-conditioning of a SSW (Coy et al., 2009); the role of gravity wave drag in the mesosphere during different winter conditions (Siskind et al., 2010); the effect of dynamical variability on the occurrence of polar mesospheric clouds (Nielsen et al., 2010; Siskind et al., 2011); and a climatology of the 2-day wave (McCormack et al., 2009, 2010). The climatologies for each single winter case of those considered in the present study have been discussed in Manney et al. (2008, 2009), Coy et al.

(2009, 2011), and Siskind et al. (2010). Here we present only the behavior of the background atmosphere that is relevant to the presence of normal modes.

We start by examining the zonal-mean winds, which influence strongly the behavior of the free modes. Figure 2 shows the zonal-mean zonal wind averaged during the four NH winters. The average is taken during the periods described in Section 2. The differences among these NH winters are subtle in the time average, but still important to notice. During the quiet winter of 2005 (Fig. 2a), the zonal circulation shows the strongest westerly flow in the stratosphere. The 20 m s^{-1} line in the winter hemisphere closes off in the lower stratosphere ($\sim 20 \text{ km}$ at 45°N) and a strong westerly flow is found in the mesosphere. The winter of 2006 (Fig. 2b) shows a zonal mean flow that is substantially weaker in the stratosphere, with the 20 m s^{-1} contour closing at about 40 km and 45°N . The winter of 2008 (Fig. 2c) is moderately disturbed as the zonal circulation weakens substantially below 40 km compared to 2005 and the 20 m s^{-1} line retreats to 25 km . On the other hand, during the winter of 2009 (Fig. 2d), the 20 m s^{-1} line retreats to even higher altitudes (above 30 km) and the mesospheric jet appears displaced and strengthened on the poleward side of the jet core.

The time-mean behavior gives only an indication of the refractive properties of the background through which planetary scale waves propagate (Dickinson, 1968), as the zonal circulation may change very rapidly during a stratospheric sudden warming (SSW). In fact, as discussed by Salby (1981a), the location of the critical line and the strength and the vertical structure of the westerly polar jet are factors that affect the presence of a normal mode. Figure 3 shows the vertical structure as a function of time of the zonal-mean zonal wind averaged poleward of 60°N from the ground to the MLT during the four winters. In order to evaluate the

state of the stratosphere, the WMO definition of SSW is adopted: a SSW occurs when the zonal-mean zonal wind at 60 N and 10 hPa becomes westward; a SSW is indicated in Fig. 3 by vertical dashed lines when it occurs in a given winter. In all years, at the beginning of winter (November and December), the polar jet strengthens up to 40-60 m s⁻¹ with a peak around the stratopause². During the quiet winter (2005; Fig. 3a) the middle atmosphere maintains an isolated polar vortex until March 2005, when the zonal wind becomes westward as equinox approaches. The winter of 2006 (Fig. 3b) shows the effect of the large SSW as westward zonal winds (about -30 m s⁻¹) appear at the stratopause in early January 2006 several days prior the SSW; the westward zonal winds descend during the following month and weaken, reaching the lower stratosphere in early February. Notice that as westward zonal winds invade the stratosphere, a strong eastward jet develops in the mesosphere during February. The winter of 2008 (Fig. 3c) is somewhat similar to the quiet winter 2005, except for brief interruptions of the eastward zonal circulation during late January and early February 2005 and the brief SSW in late February. Immediately following the SSW, the stratosphere begins to show the springtime climatology with weak eastward winds. The winter of 2009 (Fig. 3d) shows a behavior in this case more similar to the winter of 2006. Following the eastward jet established at the beginning of winter, substantial westward winds descend quickly from the mesosphere into the stratosphere in January. These anomalous westward winds continue to descend and invade the lower stratosphere, persisting as weak westward winds throughout February of 2009. As in the case of 2006, this is accompanied by a recovery of the eastward polar vortex in the mesosphere.

² Due to the limited temporal record in 2006, this behavior is less apparent in that year (Figure 3b).

Figures 2 and 3 illustrate two different types of seasonal evolution of the NH winter. The quiet winter of 2005 is characterized by strong and relatively slowly varying westerly winds throughout the middle atmosphere. At the other extreme, the highly disturbed NH winters of 2006 and 2009 show a large and rapid reversal of the zonal circulation in mid-winter, a prolonged disturbance in the lower stratosphere, and a rapid recovery in the mesosphere. Between these two winters, 2008 has a SSW of short duration in late winter, which merges with the seasonal transition to springtime. In the next Section, we examine how the presence of the normal modes is related to the meteorological behavior of a given period.

4. Spectral analysis

The spectra of westward propagating waves of wavenumber-1 for the four NH winters are investigated in this Section. We identify those spectral regions that are statistically significant using the method described in the Appendix; we then discuss the corresponding spatial structures using a coherence analysis. Specifically, we look for statistically significant wave-1 variance near 25 days, 16 days, 10 days and 5 days, the theoretical eigenperiods of the Rossby normal modes (1,4) through (1,1), respectively (Longuet-Higgins, 1968). Following on the discussion of the mean climatologies for each winter in Section 3, we expect that there will be a good deal of year-to-year variability in the observed spectra. Numerical calculations (e.g., Salby, 1981b; see his Fig. 4) show the response is broadly enhanced in different spectral ranges for each normal mode. In Table 2 we list frequency bands for each mode, labeled V1 through V4, based on guidance from Salby's numerical calculations. These bands are plausible ranges of frequency within which the 25-day through 5-day normal modes, respectively, might be expected to occur. Within these bands we apply a *band a priori* hypothesis, discussed in the Appendix, to evaluate

statistical significance. The *band a priori* hypothesis reduces the value of χ^2 required for significance within the band compared to the case with no *a priori* hypothesis; everywhere else the more stringent value of χ^2 , appropriate to the no *a priori* case, is used (see Appendix).

Figure 4 shows the wave-1 spectral amplitude as a function of frequency and altitude at 60 N for each winter. The spectral bands in Table 2 are identified by the white arrows in each panel; unshaded areas identify those spectral regions where the amplitude is large enough to reject the null hypothesis based on the *band a priori* test. For the V4 band, we find three winters with large enough amplitude to be considered statistically significant: 2005, 2008 and 2009³. The first two winters show statistically significant amplitude in the lower stratosphere and in 2008 also in the troposphere; in 2009 the amplitude is statistically significant only in mid-stratosphere, between about 20 and 40 km. The V3 band shows statistically significant amplitude in all winters over a greater or lesser altitude range depending on the year; while the largest amplitudes are found in the upper stratosphere and the lower mesosphere, statistically significant amplitudes are found also in the troposphere. The V2 band shows statistically significant amplitude during the winters of 2005, 2008 and 2009 in the upper stratosphere and lower mesosphere and also in the troposphere in 2009⁴. Finally, the V1 spectral band shows statistically significant amplitude in 2005, 2006 and 2009. The amplitude is statistically significant over a deep atmospheric layer in 2006 and 2009, but is more confined to the troposphere in 2005.

³ Statistically significant amplitude in 2006 in the troposphere appears in a continuum of decreasing magnitudes starting at zero frequency and continuing through the V4 band. Since it does not emerge as an isolated spectral peak, we do not identify it as a potential evidence of the (1,4) mode.

⁴ A sliver of statistical significance is found also in 2006 in the mesosphere around 0.11 cpd. Because of the limited spectral width of this region, we disregard it in the present discussion. It is likely that the coarse bandwidth in 2006 influences the isolation of spectral amplitude.

The spectral bands identified in Fig. 4 are used to carry out a coherence analysis, following Hayashi (1971). In the following, we discuss the spatial coherence of the amplitude and of the phase of these spectral bands and identify those cases when the spatial structure is consistent with the nominal normal mode behavior.

a) 25-day mode (V4 band)

The second anti-symmetric Rossby mode for wave-1 has a nominal period of 25 days; it is also referred to as the (1,4) mode (Salby, 1981b). Its geopotential structure with respect to latitude is anti-symmetric about the equator (Fig. 1), with three zero-crossings, one at the equator and one each in the NH and SH (see also Madden, 2007). The zonal phase speed of this wave is very slow ($\sim 9 \text{ m s}^{-1}$ at 60°). This mode is not only difficult to identify reliably in the spectrum because of distortion effects occurring with changes of the background zonal wind, but also because of the limited spectral bandwidth in any single-winter time series.

Figure 5 shows the amplitude and the phase of the band-passed geopotential heights obtained from the coherence analysis applied in the V4 band (see Table 2 and Fig. 4). Note that the amplitude and phase are shown without shading where the coherence analysis is greater than 0.9 and the shaded regions indicate those locations where the coherence squared is lower than 0.9; the reference point is at 60 N and 18 km and is indicated by a cross in each panel. The amplitude plots show the largest wave amplitude around 70 N, with substantial magnitude extending throughout the stratosphere. The winter of 2005 (Fig. 5a) has an amplitude minimum around the stratopause in winter, while in 2009 (Fig. 5e) the amplitude minimum is around 70 km, and during 2008 (Fig. 5c) the amplitude is large throughout the stratosphere and mesosphere. The

phase (Figs. 5b,d,f) conveys information on the spatial structure of the band-passed behavior. Although somewhat distorted, the phase structure in 2005 (Fig. 5b) is consistent with the (1,4) mode in the troposphere and in much of the stratosphere, with nodal points in both northern and southern sub-tropical latitudes, and a third nodal point near the equator. During 2008 (Fig. 5d), there is no indication of the expected anti-symmetric structure with three nodes anywhere. In fact, during 2008 the phase structure is mostly symmetric, particularly in the stratosphere, which is reminiscent of the (1,3) normal mode. The phase structure in 2009 (Fig. 5f) shows evidence of a phase behavior that is consistent with the nominal (1,4) mode in the troposphere. Above 20 km the phase shows a mixed response: while the NH preserves the modal response characteristic of the Rossby (1,4) mode at least up to 40 km, the SH shows a behavior closer to a (1,3) mode.

As can be evinced from Fig. 5, the identification of the mode from coherence analysis remains subject to uncertainty; for example, in 2005 the (1,4) mode with the expected meridional symmetry appears in the stratosphere. On the other hand, during 2008, while the spectral location of the statistically significant variance (V4) is similar to 2005, the phase structure is only reminiscent of the (1,3) mode with overall meridional symmetry in the stratosphere. A somewhat similar situation exists in 2009 when the structure is mostly symmetric in the stratosphere, where the largest statistical significance is calculated (Fig. 4d), but there is evidence of the nominal (1,4) normal mode behavior in the troposphere and in the lower stratosphere, where the statistical significance, however, is substantially reduced. This is an indication that the coherence analysis may be capturing a superposition of waves that include the (1,4) normal mode, but also other modes that are Doppler shifted to appear at different frequencies than expected from theory. As noted above, the difficulty with the (1,4) mode is also related to using single-winter data, which

yields a relatively broad bandwidth, hindering discrimination of different modes. Figure 5 documents a wave-1 oscillation filtered around 25 days in the NOGAPS-ALPHA analysis that, notwithstanding the prominence of the spectral peaks in some years (Fig. 4), does not always resemble the theoretical (1,4) Rossby normal mode. Our analysis of the periods analyzed by NOGAPS-ALPHA shows that the (1,4) mode is clearly present only in the troposphere and stratosphere in the dynamically undisturbed winter of 2005.

b) 16-day mode (V3 band)

The 16-day mode, or (1,3) mode, is the second symmetric Rossby mode of wavenumber 1. It has a theoretical zonal phase speed of about 14 m s^{-1} at 60° , which also makes it rather susceptible to broadening due to changes of the background winds. It was studied numerically by Salby (1981b) and Forbes et al. (1995), and extracted from re-analysis fields by Madden (2007). The meridional structure (Fig. 1) is symmetric with two nodes at low latitudes on opposite sides of the equator. Salby (1981b) noted that the spectral response under realistic background winds of the (1,3) mode is very broad, from 20 days to 12 days.

Figure 6 shows the amplitude and the phase of the band-passed behavior obtained from the coherence analysis in band V3. Again, the amplitude is shown without shading where the coherence analysis, with a reference point at 60 N and 60 km, is greater than 0.9. Note that the reference point now is located at a different altitude from that used in Fig. 5, near the amplitude maximum. In all winters the largest amplitude occurs in the upper stratosphere and the lower mesosphere. However, the largest amplitude is obtained in 2008 ($\sim 100 \text{ m}$; Fig. 6e), which is several times larger than the smallest, in 2009 ($\sim 30 \text{ m}$; Fig. 6g). In all cases, the amplitude in

the summer hemisphere is small. This contrasts with the results presented by Williams and Avery (1992), where the largest amplitude of a 16-day oscillation is found instead during local summer: this difference of the amplitude structure may reflect different excitation mechanisms operating at different times. During the winter of 2009 (Fig. 6h), the phase behavior has symmetry that is clearly consistent with the expected structure of the (1,3) normal mode in the troposphere, stratosphere and lower mesosphere; the behavior remains overall symmetric in the mesosphere, but its structure is rather distorted, with the nodal points extending to the high latitudes in both hemispheres. The winter of 2008 (Fig. 6f) also shows evidence of the (1,3) structure but only in the troposphere and the lower stratosphere. The winter of 2005 (Fig. 6b) shows symmetric behavior with nodal points around 30° in both hemispheres in the troposphere and stratosphere, although the phase tends to be somewhat distorted in the upper levels. During the winter of 2006 (Fig. 6d), the phase structure shows limited evidence of a symmetric behavior in the stratosphere and mesosphere, between ~ 20 and 70 km.

In summary, for the second symmetric Rossby mode we find evidence of a modal structure that resembles the theoretical Rossby normal mode in 2005, 2008 and 2009 in the troposphere the stratosphere, and part of the mesosphere, with more limited evidence in 2006. Note, however, that the amplitude of the band-passed behavior during the winter of 2009 (a winter with a very large and persistent SSW) is several times smaller than during the winter of 2008, reflecting the different climatology of those two winters (cf. Figs. 2 and 3). The conclusion based on the limited evidence offered by the NOGAPS-ALPHA analysis fields is that, regardless of the excitation mechanism that forces the (1,3) mode, the occurrence of the SSW in 2009 is likely responsible for the small amplitude of the normal mode in that year. This is consistent with the

presence for a prolonged period of time of westward winds in the stratosphere following the SSW.

It is worth noting that the lower stratosphere and the troposphere during the winter of 2008 show the presence of a (1,3) structure *beyond* the limits of the V3 spectral band as defined here. Evidence of this is shown in Fig. 5d for a spectral band around 25 days; another example is shown later for the V2 band in 2005 that also has a clear (1,3) modal behavior in the troposphere and the stratosphere. Such spectral broadening and Doppler shifting is also present in numerical calculations (Salby, 1981a); in the real atmosphere, the frequency overlap between normal modes makes the distinction between modes rather difficult and more complicated. It should also be noted that in these instances a finer spectral bandwidth would be of no help, as the overlapping modes are due to the physical properties of the background atmosphere as opposed to the limited length of the observational series.

c) 10-day mode (V2 band)

The 10-day normal mode, also referred to as the (1,2) Rossby mode, is the first anti-symmetric normal mode of wavenumber 1, with a single node at the equator (Fig. 1). Its zonal phase speed is about 23 m s^{-1} at 60° , which should make it less susceptible to moderately small changes of the background winds.

Figure 7 shows the amplitude and phase of the band-passed behavior in the V2 band. The largest amplitudes ($\sim 30\text{--}40 \text{ m}$) are found in 2005 and 2008 (Fig. 7a,c), and the smallest ($\sim 20 \text{ m}$) in 2009 (Fig. 7e). In all cases the amplitude reaches a maximum in mid-latitudes of the winter hemisphere. The phase structures in 2005 and 2009 (Fig. 7b,f) are symmetric and, in fact, largely

reminiscent of the (1,3) mode. Only in 2008 (Fig. 7d), is the phase structure somewhat reminiscent of the (1,2) mode in the troposphere. If one neglects the behavior at high southern latitudes, the two hemispheres show anti-symmetric behavior that is separated by a zero phase line approximately at the equator. Note that above 20 km, the behavior in 2008 is largely symmetric, as for the (1,3) mode. The prominent presence of symmetric structures in particular in the stratosphere and mesosphere suggests frequency overlap between different normal modes, following spectral broadening and Doppler shifting due to the unsteadiness of the background atmosphere.

d) 5-day wave (V1 band)

The 5-day wave, also known as the (1,1) mode, is the first symmetric Rossby mode. Salby (1981b) discusses the spectral breadth of this mode, identifying a 5-day type response between 4 and 6 days. Wu et al. (1994) found evidence in satellite data of the (1,1) mode at about 6 days (~ 0.16 cpd) in HRDI (High Resolution Doppler Imager) data, and Pancheva et al. (2010) show that a westward wave-1, 5.5-day oscillation is present in SABER data. The signature of a 5-day wave has also been found in tracers (Pendlebury et al., 2008). The (1,1) mode is symmetric and lacks nodal points in the meridional direction (see Fig. 1). The theoretical mode has a sufficiently fast horizontal phase speed (46 m s^{-1} at 5 days; 33 m s^{-1} at 7 days) that it should be less susceptible to variations of the underlying winds, relative to the slower modes.

Statistically significant spectral peaks at around 0.2 cpd are found in the analysis spectra in 2005, 2006 and 2009 (Fig. 4). The coherence analysis yields the amplitude and phase plots shown in Fig. 8. In 2005 (Fig. 8a) and 2006 (Fig. 8c), two distinct amplitude peaks are found, in

the winter (northern) hemisphere around 70 N and in the summer (southern) hemisphere in the MLT region around 60 N. The amplitude in 2009 (Fig. 8e) instead has a broad peak in the MLT with no indication of a preferential latitude. This last result does not agree with numerical calculations (Salby, 1981b), which have shown a more pronounced amplitude in the summer (southern) hemisphere. The different location of the amplitude maxima in 2009 between the observational analysis and theoretical numerical calculations is probably indicative of a forcing mechanism operating in the winter (northern) hemisphere: a larger amplitude will generally occur near the location where the forcing is present. The accompanying phase structures show a mode whose phase is uniform horizontally and with very long vertical wavelength during 2005 (Fig. 8b) and 2009 (Fig. 8f), confirming the presence of a (1,1) Rossby normal mode in this winter. The phase structure in 2006 is reminiscent of a (1,1) mode only in the upper mesosphere. Large amplitudes in the southern (summer) hemisphere are present also in numerical calculations (e.g., Salby, 1981b; see his Fig. 6), and it is worth noting that those amplitudes in 2005 and 2006 may exert a substantial control over the occurrence of polar mesospheric clouds (Nielsen et al., 2010); the wave amplitude can be enhanced locally by the occurrence of dynamical instability associated with large meridional gradients of the zonal mean wind and the associated temperature fluctuation can favor the formation of clouds.

6. Relation to SSW

The spatial structures of the band-passed wave-1 geopotential anomalies in the analysis fields, discussed in the previous section, illustrate the occasional presence of normal modes during four recent winters. Based on the limited evidence presented in this study, the winters with SSW do not seem to favor the amplification of normal modes, contrary to some previous

findings (e.g., Pancheva et al. 2008). The two winters with large SSW (2006 and 2009) show limited evidence of slow normal modes [e.g., the (1,4) mode], and the amplitude of the modes that can be identified is substantially smaller than during the winters (2005, 2008), which are relatively quiet dynamically. The only wave-1 normal mode that is clearly identifiable during most winters is the 16-day wave (V3 band), the mode most typically reported in observations during SSWs (e.g., Dowdy et al. 2004).

The fact that the normal modes are less likely to be found in winters with SSW is not inconsistent with theory. Salby (1981b) shows that normal modes should appear more prominently when the zonal circulation is relatively undisturbed and eastward. The amplitude of the normal modes is substantially biased toward the winter hemisphere near solstice when westward winds are predominant in the summer hemisphere. This picture is complicated in real atmospheric situations where the zonal circulation is far from being steady, which is one of the assumptions in Salby's study, and the presence of forced waves may result in a reversal of the zonal circulation, inhibiting the presence of westward propagating normal modes in the stratosphere. Gravity-wave drag further complicates normal mode structures in the mesosphere and lower thermosphere (e.g., Forbes et al. 1995). Therefore, the absence of some Rossby normal modes in the winters with SSWs may be the result of the occurrence of disturbed periods during which the zonal circulation reverses and prevents the slower modes from reaching the middle atmosphere.

By way of example, we show the intrinsic frequency corresponding to the V3 (12-25 day) band in 2005 and 2009 in Figure 9. Figure 9a shows that the intrinsic frequency in 2005 is quite similar to that obtained by Salby (1981b, his Fig. 8d) using a numerical model that employs a

stationary wind distribution. The intrinsic frequency is negative (i.e., the zonal phase speed is westward) in the winter hemisphere with values increasingly more westward in the upper stratosphere and lower mesosphere. A critical line is found in the summer hemisphere; starting from the stratopause at the South Pole, it extends to the equator in the upper stratosphere. The intrinsic frequency during the highly disturbed winter of 2009 prior to the warming (averaged between November 1 2008 through January 23 2009; Fig. 9b) is similar to that shown in 2005 because the zonal circulation during this time in 2009 is still westerly in the winter hemisphere as it is the case of the winter of 2005. However, the averaged intrinsic frequency after the SSW (between January 24 2009 and 15 February 2009, Fig. 9c) shows a substantially different structure; the intrinsic frequency is weakly westward below 40 km in the winter hemisphere and large westward values are found only in the upper mesosphere.

In a situation like that found in 2009 (Fig. 9c), slow normal modes, like (1,4) and (1,3), are inhibited from propagating in the stratosphere due to the presence of a critical line. Particularly for the (1,3) mode, evidence of the high susceptibility of the slow modes to the background wind configurations is also reported in Lou et al. (2000) and Namboothiri et al. (2002). At the same time, faster modes such as (1,1) are less affected by changes of the zonal winds even in a highly disturbed winter, such as 2009. Figure 10 shows the intrinsic frequency for the (1,1) mode averaged prior to the SSW and after the SSW (same averaging periods as in Fig. 9b,c). The resulting maps of the intrinsic frequency in the two periods are similar: although the intrinsic frequency is somewhat less westward in the lower stratosphere during the second period (Fig. 10b) compared to the earlier period (Fig. 10a), it remains substantially westward globally.

6. Summary and Conclusions

Using global observational meteorological analyses that extend from the surface to the upper mesosphere and lower thermosphere, we have isolated the spectral band-passed behavior of the gravest zonal waves corresponding to the eigenfrequencies of the (1,4), (1,3), (1,2) and (1,1) normal modes during four recent winters. The spectral locations of the response are near the eigenfrequencies of those modes, but substantial broadening around those frequencies is observed and inferred. This is to be expected because, as the background atmosphere changes, the response broadens and shifts from the theoretical eigenfrequency (Salby, 1981a). It should also be borne in mind that the resulting response calculated using atmospheric data always contains a mixture of waves that may confound the detection and identification of the normal modes. While we cannot offer a proof, we propose that this mixture of waves results from the spectral broadening that is caused by the non-stationarity of the background atmosphere. This difficulty is compounded by the limited record length, which coarsens the bandwidth and the ability to isolate those modes clearly.

Other authors have attempted to isolate normal modes in atmospheric data. The present work has a different emphasis from those studies that focus on lower atmospheric behavior (e.g., Madden, 2007), or those that investigate the normal modes during specific wintertime conditions (Smith, 1985; Forbes et al., 1995). Instead, we exploit the deep atmospheric coverage of the NOGAPS-ALPHA data assimilation products to investigate the structure of the normal modes up to the lower thermosphere during four northern hemisphere winters: a quiet winter (2005), a disturbed winter (2006), a moderately disturbed winter (2008), and a highly disturbed winter (2009). At the same time, an evident shortcoming of this study is that the conclusions drawn here

apply strictly speaking only to those winters. A more comprehensive climatology of these normal modes and their relevance during different atmospheric conditions is yet to be done but is beyond the scope of this study.

We offer the following conclusions:

- Statistically significant spectral peaks at the spectral locations of the (1,4), (1,3), (1,2) and (1,1) normal modes are found in some winters, but with markedly different amplitudes. The geopotential amplitudes are largest in the mid-latitude winter upper stratosphere and lower mesosphere. A close inspection of the meridional behavior (via coherence analysis) yields a structure that is only occasionally reminiscent of the theoretical normal modes (Salby 1981). The amplitude of the slower modes tends to be reduced during dynamically disturbed winters (2006 and 2009). Particularly noticeable is the presence of a symmetric structure beyond 0.06 cpd that is reminiscent of the (1,3) normal mode. On the other hand, the (1,2) anti-symmetric behavior is missing from most of the years analyzed, emerging with very modest amplitude in the troposphere only in the winter of 2008.

- The (1,1) mode, or 5-day wave, is present with statistically significant amplitude during three winters (2005, 2006, and 2009). Particularly during 2009, the amplitude is significantly different from the AR1 spectrum over a deep atmospheric layer from the lower stratosphere to the upper mesosphere. This wave mode has a relatively high zonal phase speed, and it is not affected substantially by the changes of the background atmosphere during winter. The resulting spatial structure is very close to that predicted by theory for the (1,1) mode. We found that the

amplitude in the summer MLT region is amplified in some years; this amplification has been suggested as a cause for the observation late in the season of polar mesospheric clouds.

- The slower modes, that is, the (1,3) and (1,4) normal modes, are more likely to be affected by the transient behavior of the background winds in particular during disturbed wintertime periods. In fact, we present some evidence of these modes in the winter of 2005, which is quiet. In particular for the (1,4) mode, its presence is limited to the lower atmosphere.

- There is no evidence that the occurrence of a SSW amplifies normal modes, or vice-versa. In fact, when a SSW is so large and persistent as to eliminate the eastward winds in the extra-tropical stratosphere of the winter hemisphere, a critical line can appear for the slow normal modes in the lower stratosphere that prevents them propagating to higher altitudes. It is perhaps for this reason that the normal modes are seen more clearly in the winter of 2005, which is the most dynamically quiet of all the winters analyzed and included no SSW.

- We note that the modes identified here have generally small time-mean amplitude in all of the winters analyzed. In particular, the (1,3) mode, or 16-day wave, has winter-mean amplitudes (Fig. 6) that do not exceed about 100 m. This is much smaller than the transient wave amplitudes attributed to the 16-day wave in the winter of 1979 prior to the occurrence of a major SSW (as much as several hundred meters at 1 hPa; see, e.g., Madden and Labitzke, 1981; Smith 1985). The discrepancy may arise from the way in which transient waves are characterized. In this study, we identify the (1,3) normal mode (and other normal modes) with the variance within a band predicted by theory and judged to be statistically significant, as explained in Section 4. On the other hand, the studies cited above define transient waves as the departure from the time

mean for the period of analysis. For data with short records, this is unavoidable, but it conflates transient variance at all frequencies. If one defines the normal modes in terms of statistically significant response only within the theoretical bands of frequency where they are expected to occur, one must conclude that they achieve only modest amplitudes and may not play an important role in the generation of SSW events. In fact, recent studies of the 16-day wave yield amplitudes more in line with our results. For example, Pogoreltsev et al (2009) estimate 16-day wave geopotential amplitudes of about 30 m at 30 hPa from NCAR/NCEP reanalysis data, which is comparable to the results shown in our Fig. 6. Lott et al. (2009) used ERA-40 data to construct composite episodes of strong activity in the period band 7-30 days, and estimated amplitudes of 30 m in the lower stratosphere (50 hPa). This is larger than what we obtain at that level by at least a factor of 2, but our results are wintertime means, whereas Lott et al's results emphasize periods of high 16-day wave activity. When we compute the time-dependent amplitude of the 16-day wave in the winter of 2007-2008, we find values at 50 hPa (not shown) that range between 10 and 30 m.

The limited frequency bandwidth due to in single-winter's length of data may have limited our ability to reliably distinguish between wave modes when closely located in spectral space. At the same time, we find a mixture of modes with overlapping spectral bands and in this case a finer bandwidth is of limited help. In contrast to numerical, steady-state calculations in a uniform background state, the real atmosphere contains background winds and temperatures that are neither steady nor uniform, and would be expected to broaden the normal mode responses around their theoretical frequencies. Evidence presented in this study suggests that wave modes can be Doppler-shifted and spectrally broadened to overlap adjacent modes.

Acknowledgments. The authors thank S.D. Eckermann and J.P. McCormack for comments and discussions on this manuscript. F. Sassi and K.W Hoppel were supported by NASA's Heliophysics Guest Investigator Program (contract NNH09AK641) and by the Office of Naval Research through NRL's base 6.1 and 6.2 research programs. The National Center for Atmospheric Research is sponsored by the National Science Foundation. This work was supported in part by a grant of computer time from the DOD High Performance Computing Modernization Program at the Navy's DOD Supercomputing Resources Center.

Appendix: Statistical significance of signals in selected frequency bands using a “band *a priori*” hypothesis

In the following we draw from the discussion of AR1 processes found in Wilks (2006). An autoregressive process of the first order is defined as

$$x_{t+1} - \mu = \rho(x_t - \mu) + \varepsilon_{t+1} \quad (\text{A.1})$$

where x_t and x_{t+1} are the values of the predicted time series at times t and $t + 1$, μ is the mean of the time series, ρ is the lag-1 auto-correlation parameter, and ε_{t+1} is a random (uncorrelated) quantity at time $t+1$ with zero mean and variance σ_ε^2 equally distributed at all frequencies. The spectrum of the autoregressive process (A.1) is

$$S(\omega) = \frac{2\sigma_\varepsilon^2 / N}{1 + \rho^2 - 2\rho \cos(\omega)} \quad (\text{A.2})$$

where ω is the frequency in rad s⁻¹, N is the number of data points. Eq. (A.2) represents the background spectrum, which we use it to define the null hypothesis. Wilks (2006) provides a simple formula to determine how large the spectral amplitude at frequency ω_i needs to be in order to reject the null hypothesis: the squared amplitude Ψ_i^2 associated with the i -th spectral component at frequency ω_i is deemed statistically significant at level $(1-\alpha)$ if

$$\frac{v\Psi_i^2}{S(\omega_i)} > \chi^2 \quad (\text{A.3})$$

where χ^2 is the value of the chi-squared distribution corresponding to a statistical significance level of $(1-\alpha)$ with v degrees of freedom.

Following Fisher (1929), Wilks (2006) notes that, without an *a priori* hypothesis on the spectral location of the peaks of variance, one needs to use a more stringent level of statistical

significance in (A.3) than α . In essence, without knowing *a priori* where the spectral peaks are located, it is necessary to evaluate the statistical significance at a value of α^* given by

$$\alpha^* = \alpha / K^* \quad (\text{A.4})$$

where K^* is the effective number of independent frequencies; that is, $K^*=K/S_f$, where K is the number of frequencies in a band of interest and S_f is the number of frequencies that are averaged to smooth the periodogram. All spectra in this study are obtained by smoothing the periodogram using a 5-point boxcar average. For example, for a 90% confidence level, $\alpha=0.1$ and taking $K=180$ and $S_f=5$, then $K^*=36$ and $\alpha^*=0.003$, which implies that an effective confidence level of 99.7% is required to reject the null hypothesis with 90% confidence. The value of χ^2 in (A.3) is determined from the value of the chi-squared probability distribution corresponding to $(1-\alpha^*)$ and 10 degrees of freedom (2 degrees of freedom per spectral component).

In order to apply the test (A.3), one needs to evaluate (A.2), where only two parameters are unknown: the “white noise” variance σ_ε^2 and the auto-correlation ρ at lag-1. The auto-correlation is determined from the spectral coefficients using the Wiener-Khinchin theorem, while the white noise variance is easily obtained from (A.1) by squaring and averaging both sides of the equation to obtain

$$\sigma_\varepsilon^2 = (1 - \rho^2) \sigma_x^2 \quad (\text{A.5})$$

where σ_x^2 is the variance of the time series (see also Wilks, 2006).

While an evaluation of the spectra without an *a priori* hypothesis is certainly possible, it is unnecessarily restrictive, since in fact we have some *a priori* knowledge of where the normal mode are expected to occur and also of the associated spectral uncertainty. The latter may be estimated from the spectral range obtained from the numerical calculations of Salby (1981b) and summarized for each mode in Table 2. Thus, the V3 spectral band has about 8 spectral frequencies with a bandwidth of 180 days. Accounting for the spectral smoothing ($S_f=5$), the effective number of frequencies (K^* in Eq. A.4) is then about 1.6, which requires a critical value

of χ^2 corresponding to a 94% probability to reject the null hypothesis with a confidence of 90%. It should be noted that a *band a priori* hypothesis can be evaluated with this reduced level of confidence only in the spectral band for which we have an hypothesis that the normal mode may exist; outside that spectral range, one needs to use the *no a priori* hypothesis (A.4) which requires instead a value of χ^2 corresponding to 99.7%, as discussed above.

The RMS amplitude at 60 N for the null hypothesis thus estimated is shown in Fig. A1 for the winter of 2005 using the 90% level of statistical confidence. A *band a priori* hypothesis is used only in the V3 spectral range (see Table 2) for this example, while the *no a priori* hypothesis is used in the rest of the spectrum; this explains the apparent discontinuity in amplitude between the vertical black lines, which delimit the V3 spectral band and the rest of the spectral amplitudes. Notice how narrowly peaked the null spectrum is below 20 km as opposed to the much broader spectrum above that elevation. This reflects the high auto-correlation of the time series in the troposphere and lowermost stratosphere, and the reduced auto-correlation and larger white noise variance in the rest of the middle atmosphere.

References

- Baker, N.L., et al., 2007. An overview of the NRL Atmospheric Variational Data Assimilation (NAVDAS) and NAVDAS-AR (Accelerated Representer) Systems. In: 18th AMS Conference on Numerical Weather Prediction, 25–29 June, ParkCity, UT, Paper 2B.1, 6pp. (Available at: <http://ams.confex.com/ams/pdfpapers/124031.pdf>).
- Coy, L., S.D. Eckermann and K.W. Hoppel, 2009. Planetary wave breaking and tropospheric forcing as seen in the stratospheric sudden warming of 2006. *J. Atmos. Scie.*, **66**, 495-507.
- Coy L., S.D. Eckermann, K.W. Hoppel, and F. Sassi, 2011. Mesospheric precursors to the major stratospheric sudden warming of 2009: Validation and dynamical attribution using a ground-to-edge-of-space data assimilation system. *J. Adv. Model. Earth Sys.*. Submitted.
- Daley, R., and E. Barker, 2001. NAVDAS: formulation and diagnostics. *Mon. Wea. Rev.*, **129**, 869-883.
- Day, K.A. and N.J. Mitchell, 2010. The 16-day wave in the Arctic and Antarctic mesosphere and lower thermosphere. *Atmos. Chem. Phys.*, **10**, 1461-1472.
- Dickinson, R.E., 1968. Planetary Rossby waves propagating vertically through weak westerly wind wave guides. *J. Atmos. Scie.*, **25**, 984-1002.
- Dowdy, A.J., R.A. Vincent, D.J. Murphy, M. Tsutsumi, D.M. Riggin, M.J. Jarvis, 2004. The large-scale dynamics of the mesosphere-lower thermosphere during the Southern Hemisphere stratospheric warming of 2002. *Geophys. Res. Lett.*, **31**, doi:10.1029/2004GL020282.
- Eckermann, S.D., K.W. Hoppel, L. Coy, J.P. McCormack, D.E. Siskind, K. Nielsen, A. Kochenash, M.H. Stevens, C.R. Englert, W. Singer, and M. Hervig, 2009. High-altitude data assimilation system experiments for the northern summer mesosphere season of 2007, *J. Atmos. Sol.-Terr. Phys.*, **71**, 531-551.

- Eliassen, E. and B. Machenhauer, 1965. A study of the fluctuation of the atmospheric planetary flow patterns represented by spherical harmonics. *Tellus*, **17**, 220-238.
- Eliassen, E. and B. Machenhauer, 1969. On the observed large-scale atmospheric wave motions. *Tellus*, **21**, 149-165.
- Espy P.J., J. Stegman, and G. Witt, 1997. Interannual variations of the quasi-16-day oscillation in the polar summer mesospheric temperature. *J. Geophys. Res.*, **102**, 1983-1990.
- Fisher, R.A., 1929. Tests of significance in harmonic analysis. *Proc. Royal Soc. Lond. Series A*, **125**, 54-59.
- Forbes, J.M., M.E. Hagan, S. Miyahara, F. Vial, A.H. Manson, C.E. Meek, and Y.I Portnyagin, 1995. Quasi 16-day oscillation in the mesosphere and lower thermosphere. *J. Geophys. Res.*, **100**, 9149-9163.
- Garcia, R.R., D.R. Marsh, D.E. Kinnison, B.A. Boville, and F. Sassi, 2007. Simulation of secular trends in the middle atmosphere, 1950-2003. *J. Geophys. Res.*, **112**, doi: 10.1029/2006JD007485.
- Hayashi, Y., 1971. A generalized method of resolving disturbances into progressive and retrogressive waves by space Fourier and time cross-spectral analyses. *J. Meteor. Soc. Jap.*, **49**, 125-128.
- Hirooka, T. and I. Hirota, 1985. Normal mode Rossby waves observed in the upper stratosphere. Part II: Second antisymmetric and symmetric modes of zonal wavenumbers 1 and 2. *J. Atmos. Sci.*, **42**, 536-548.
- Hogan, T.F. and T.E. Rosmond, 1991. The description of the navy operational global atmospheric prediction system's spectral forecast model. *Mon. Weather Rev.*, **119**, 1786-1815.

- Hoppel, K.W., N.L. Baker, L. Coy, S.D. Eckermann, J.P. McCormack, G.E. Nedoluha, and D.E. Siskind, 2008. Assimilation of stratospheric and mesospheric temperatures from MLS and SABER into a global NWP model. *Atmos. Chem. Phys.*, **8**, 6103-6116.
- Longuet-Higgins, M.S., 1968. The eigenfunctions of Laplace's tidal equations over a sphere. *Phil. Trans. Roy. Soc. Lond., Ser. A*, **262**, 511-607.
- Lou, Y., A.H. Manson, C.E. Meek, C.K. Meyer, and J.M. Forbes, 2000. The quasi 16-day oscillations in the mesosphere and lower thermosphere at Saskatoon (52°N, 107°W), 1980-1996. *J. Geophys. Res.*, **105**, 2125-2138.
- Lott, F., J. Kuttippurath, and F. Vial, 2009. A climatology of the gravest waves in the equatorial lower and middle stratosphere: Method and results for the ERA-40 re-analysis and the LMDz GCM. *J. Atmos. Sci.*, **66**, 1327-1346.
- Madden, R.A., 1978. Further evidence of traveling planetary waves. *J. Atmos. Sci.*, **35**, 1605-1618.
- Madden, R.A., 2007. Large-scale, free Rossby waves in the atmosphere - an update. *Tellus*, **59A**, 571-590.
- Madden, R., and P. Julian, 1972. Further evidence of global scale, 5-day pressure waves. *J. Atmos. Sci.*, **29**, 1464-1469.
- Madden, R., and K. Labitzke, 1981. A free Rossby wave in the troposphere and stratosphere during January 1979. *J. Geophys. Res.*, **86**, 1247-1254.
- Manney, G.L. et al., 2008. The evolution of the stratopause during the 2006 major warming: Satellite data and assimilated meteorological analyses. *J. Geophys. Res.*, **113**, doi: 10.1029/2007JD009097.
- Manney, G.L., M.J. Schwartz, K. Kruger, M.L. Santee, S. Pawson, J.N. Lee, W.H. Daffer, R.A. Fuller, and N.J. Livesey, 2009. Aura Microwave Limb Sounder observations of dynamics and

- transport during the record-breaking 2009 Arctic stratospheric major warming. *Geophys. Res. Lett.*, **36**, doi: 10.1029/2009GL038586.
- McCormack, J.P., S.D. Eckermann, D.E. Siskind, T.J. McGee, 2006. CHEM2D-OPP: A new linearized gas phase ozone chemistry parameterization for high-altitude NWP and climate model. *Atmos. Chem. Phys.*, **6**, 4943-4972.
- McCormack, J.P., K.W. Hoppel, and D.E. Siskind, 2008. Parameterization of middle atmospheric water vapor photochemistry for high-altitude NWP and data assimilation. *Atmos. Chem. Phys.*, **8**, 7519-7532.
- McCormack, J.P., L. Coy, K.W. Hoppel, 2009. Evolution of the quasi 2-day wave during January 2006. *J. Geophys. Res.*, **114**, doi:10.1029/2009JD012239.
- McCormack, J.P., S.D. Eckermann, K.W. Hoppel, and R.A. Vincent, 2010. Amplification of the quasi-two day wave through nonlinear interaction with the migrating diurnal tide. *Geophys. Res. Lett.*, **37**, doi:10.1029/2010GL043906.
- Meyer, C. and J.M. Forbes, 1997. A 6.5-day westward propagating wave: Origin and characteristics. *J. Geophys. Res.*, **102**, 26,173-26,178.
- Namboothiri, S.P., P. Kishore, and K. Igarashi, 2002. Climatological studies of the quasi 16-day oscillations in the mesosphere and lower thermosphere at Yamagawa (31.2°N 130.6°E), Japan. *Ann. Geophys.*, **20**, 1239-1246.
- Nielsen, K., D.E. Siskind, S.D. Eckermann, K.W. Hoppel, L. Coy, J.P. McCormack, S. Benze, C.E. Randall, and M.E. Hervig, 2010. Seasonal variation of the quasi 5 day wave: Causes and consequences for polar mesospheric cloud variability in 2007. *J. Geophys. Res.*, **115**, doi: 10.1029/2009JD012676.
- Pancheva, D. et al., 2008. Planetary waves in coupling the stratosphere and mesosphere during the major stratospheric warming in 2003/2004. *J. Geophys. Res.*, **113**, doi: 10.1029/2007JD009011.

- Pancheva, D., P. Mukhtarov, B. Andonov, and J.M. Forbes, 2010. Global distribution and climatological features of the 5-6-day planetary waves seen in the SABER/TIMED temperatures (2002-2007). *J. Atmos. Sol.-Terr. Phys.*, **72**, 26-37.
- Pendlebury, D., T.G. Shepherd, M. Pritchard, and C. McLandress, 2008. Normal modes Rossby waves and their effect on chemical composition in the late summer stratosphere. *Atmos. Chem. Phys.*, **8**, 1925-1935.
- Pogoreltsev, A.I., A. Yu. Kanukhina, E.V. Suvorova, and E.N. Savenkova, 2009. Variability of planetary waves as a signature of possible climatic changes. *J. Atmos. Sol.-Terr. Phys.*, **71**, 1529-1539.
- Salby, M.L., 1981a Rossby normal modes in nonuniform background configurations. Part I: Simple Fields. *J. Atmos. Sci.*, **38**, 1803-1826.
- Salby, M.L., 1981b Rossby normal modes in nonuniform background configurations. Part II: Equinox and solstice conditions. *J. Atmos. Sci.*, **38**, 1827-1840.
- Salby, M.L., 1984. Transient disturbances in the stratosphere: implications for theory and observing systems. *J. Atmos. Terr. Phys.*, **46**, 1009-1047.
- Siskind, D.E., S.D. Eckermann, J.P. McCormack, L. Coy, K.W. Hoppel, and N.L. Baker, 2010. Case studies of the mesospheric response to recent minor, major and extended stratospheric warmings. *J. Geophys. Res.*, **115**, doi:10.1029/2010JD014114.
- Siskind, D.E., M.H. Stevens, M. Hervig, K. Hoppel, F. Sassi, C. Englert, A.J. Kochenash, 2011. Consequences of recent Southern Hemisphere winter variability on polar mesospheric clouds. *J. Atmos. Sol-Terr. Phys.* Submitted.
- Smith, A.K., 1985. Wave transience and wave-mean flow interaction caused by the interference of stationary and traveling waves. *J. Atmos. Sci.*, **42**, 529-535.

- Stevens, M.H. et al., 2010. Tidally induced variations of polar mesospheric cloud altitudes and ice water content using a data assimilation system. *J. Geophys. Res.*, **115**, doi: 10.1029/2009JD013225.
- Williams, C.R. and S.K. Avery, 1992. Analysis of long-period waves using the mesosphere-stratosphere-troposphere radar at Poker Flat, Alaska. *J. Geophys. Res.*, **97**, 20,855-20,861.
- Wilks, D.S., 2006. Statistical methods in the atmospheric sciences. Academic Press, Burlington (MA), 627 pp.
- Wu, D.L., P.B. Hays, and W.R. Skinner, 1994. Observations of the 5-day wave in the mesosphere and lower thermosphere. *Geophys. Res. Lett.*, **21**, 2733-2736.

Table 1. Analyzed time periods

Winter	Date Range	No. of Days
2005	20 Nov 2004 to 30 March 2005	131
2006	20 December 2005 to 20 March 2006	90
2008	1 Nov 2007 to 31 March 2008	152
2009	1 Nov 2008 to 30 April 2009	181

Table 2. Spectral bands

Band Label	Frequency range (cpd)	Period Range (days)
V4	0.030-0.050	20-33
V3	0.040-0.085	12-25
V2	0.090-0.120	8-11
V1	0.160-0.220	4.5-6.25

Figure Captions

Figure 1. Normalized amplitude of the geopotential as a function of latitude for the wave number 1 Rossby normal modes. From left to right, the 25-day wave (1,4) mode, the 16-day wave (1,3) Rossby mode, the 10-day wave (1,2) Rossby mode, and the 5-day wave (1,1) Rossby mode. Figure is adapted from Madden (2007).

Figure 2. Altitude-latitude, time mean zonal mean zonal wind for the winters of (a) 2005, (b) 2006, (c) 2008, and (d) 2009. Contour interval is 10 m s^{-1} . See Table 1 for the list of the analyzed time periods corresponding to each winter.

Figure 3. Daily values of the polar cap average (latitude greater than 60°N) of the zonal mean zonal wind as a function of altitude and time. The daily values are plotted in the range from November 1 through April 30 for each case; months are highlighted by the letters at the bottom of each panel, with the first day of the month shown by the heavy vertical lines. The dashed vertical line locates the SSW where appropriate. Negative values (westward zonal wind) are shaded and the associated contours are shown in white. Contour interval is 10 m s^{-1} .

Figure 4. Amplitude spectrum of the wave-1 westward propagating modes as a function of altitude at 60°N . (a) 2005; (b) 2006; (c) 2008; (d) 2009. Color table is shown at the bottom as the \log_{10} of the amplitude in meters. Grey-ed out areas are not statistically significant based on the application of the band a priori hypothesis.

Figure 5. Amplitude and phase obtained from the coherence analysis of the V4 bands in Fig. 4. (a)-(b) are for 2005; (c)-(d) for 2008; (e)-(f) 2009. Unshaded areas have coherence above 0.9 with a reference point at 60°N and 18 km. Contour interval is 5 m for the amplitude and 30° for the phase.

Figure 6. As in Fig. 5 but for the V3 band. (a) 2005, (b) 2006, (c) 2008, and (d) 2009. Contour interval is 10 m for the amplitude. Reference point is at 60°N and 60 km, indicated by the black cross.

Figure 7. As in Fig. 5 but for the V2 bands. (a)-(b) 2005; (c)-(d) 2008; (e)-(f) 2009. Contour interval is 10 m for the amplitude in panels (a) and (c), and 5 m in panel (e). Contour interval for the phase 30° throughout. Reference point is at 60 N and 60 km, indicated by the black cross.

Figure 8. As in Fig. 5 but for the V1 band. (a-b) 2005, (c-d) 2006; (e-f) 2009. Contour interval for the amplitude plots is 2 m. Contour interval for the phase 30° throughout.

Figure 9. Intrinsic frequency (cpd) for the V3 band (a) during the entire winter of 2005; (b) in 2009 up to the day prior the SSW; (c) in 2009 from the day of the SSW through February 15 2009. Contour interval is 0.1 cpd.

Figure 10. Intrinsic frequency (cpd) for the V1 band during the winter of 2009, (a) for days up to the day prior the SSW; (b) for days from the SSW to February 15 2009. Contour interval is 0.1 cpd.

Figure A1. Amplitude of the null hypothesis obtained from the AR1 spectrum at wavenumber-1 and 60 N during the winter of 2005, using a 90% confidence interval. A *band a priori* hypothesis is used in the spectral range V3 (~ 0.07 cpd to 0.093 cpd; vertical black lines), but a *no a priori* hypothesis is used outside that range. The color bar at the bottom shows the \log_{10} of the amplitude.

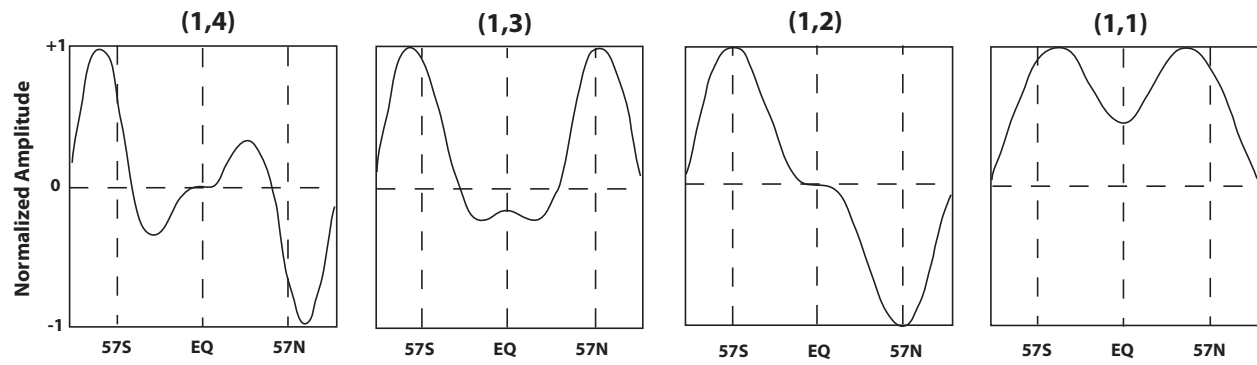


Figure 1. Normalized amplitude of the geopotential as a function of latitude for the wave number 1 Rossby normal modes. From left to right, the 25-day wave (1,4) mode, the 16-day wave (1,3) Rossby mode, the 10-day wave (1,2) Rossby mode, and the 5-day wave (1,1) Rossby mode. Figure is adapted from Madden (2007).

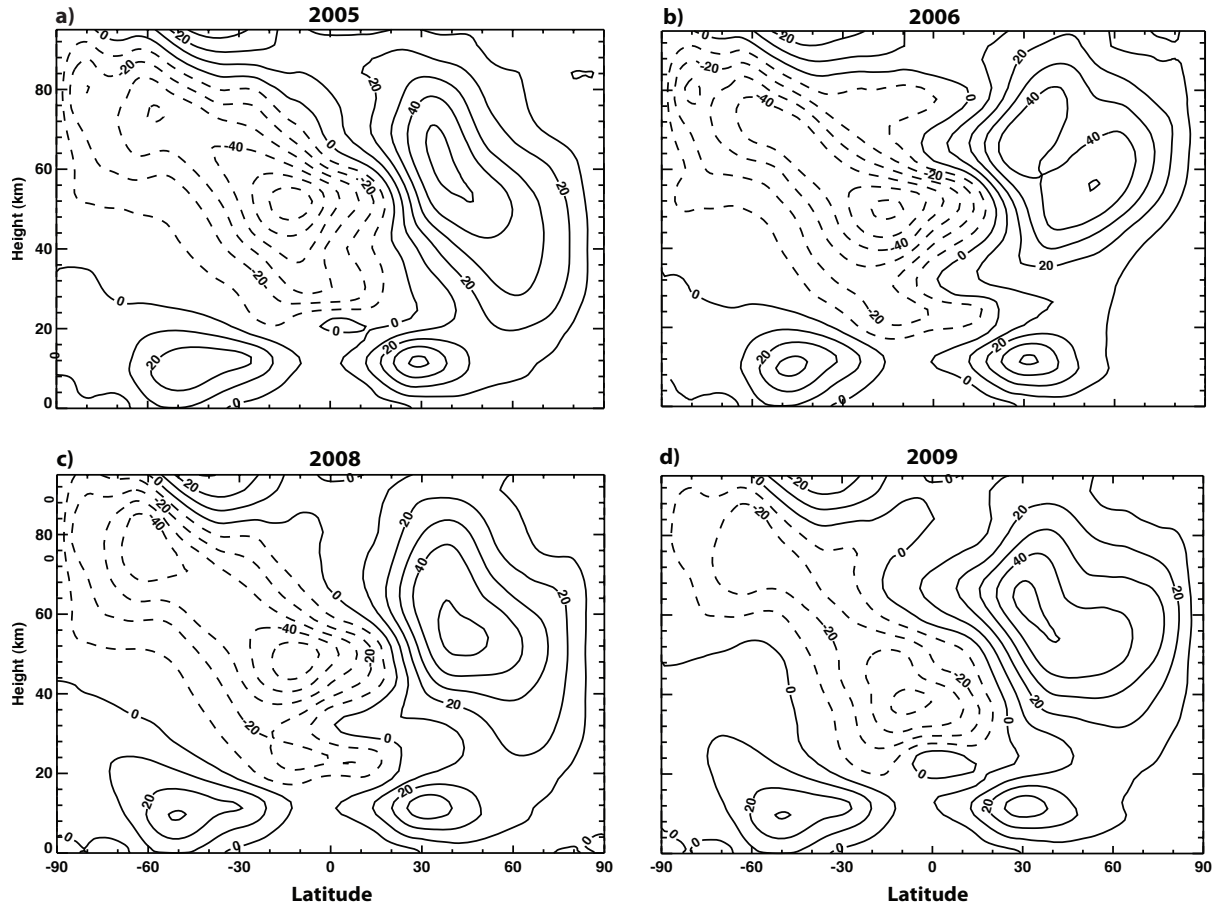


Figure 2. Altitude-latitude, time mean zonal mean zonal wind for the winters of (a) 2005, (b) 2006, (c) 2008, and (d) 2009. Contour interval is 10 m s^{-1} . See Table 1 for the list of the analyzed time periods corresponding to each winter.

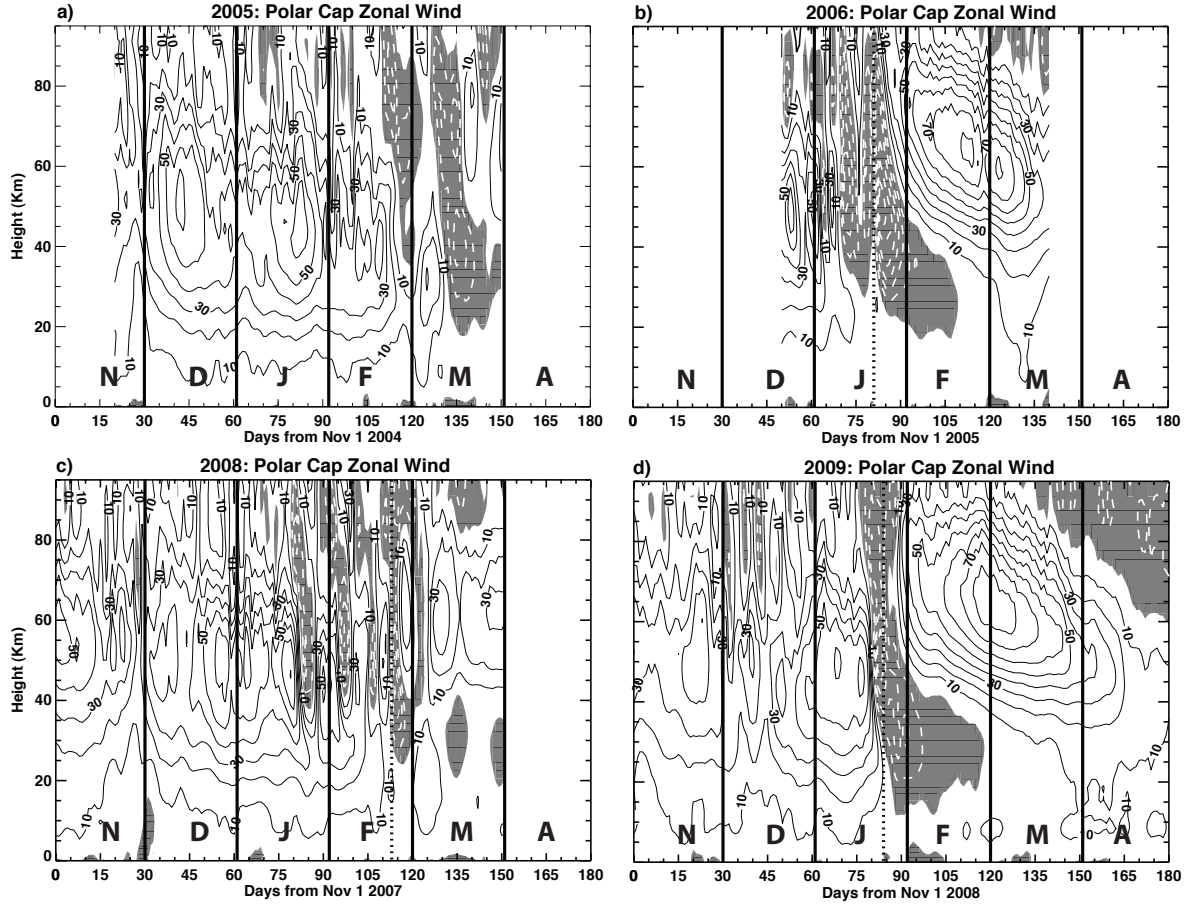


Figure 3. Daily values of the polar cap average (latitude greater than 60 N) of the zonal mean zonal wind as a function of altitude and time. The daily values are plotted in the range from November 1 through April 30 for each case; months are highlighted by the letters at the bottom of each panel, with the first day of the month shown by the heavy vertical lines. The dashed vertical line locates the SSW where appropriate. Negative values (westward zonal wind) are shaded and the associated contours are shown in white. Contour interval is 10 m s⁻¹.

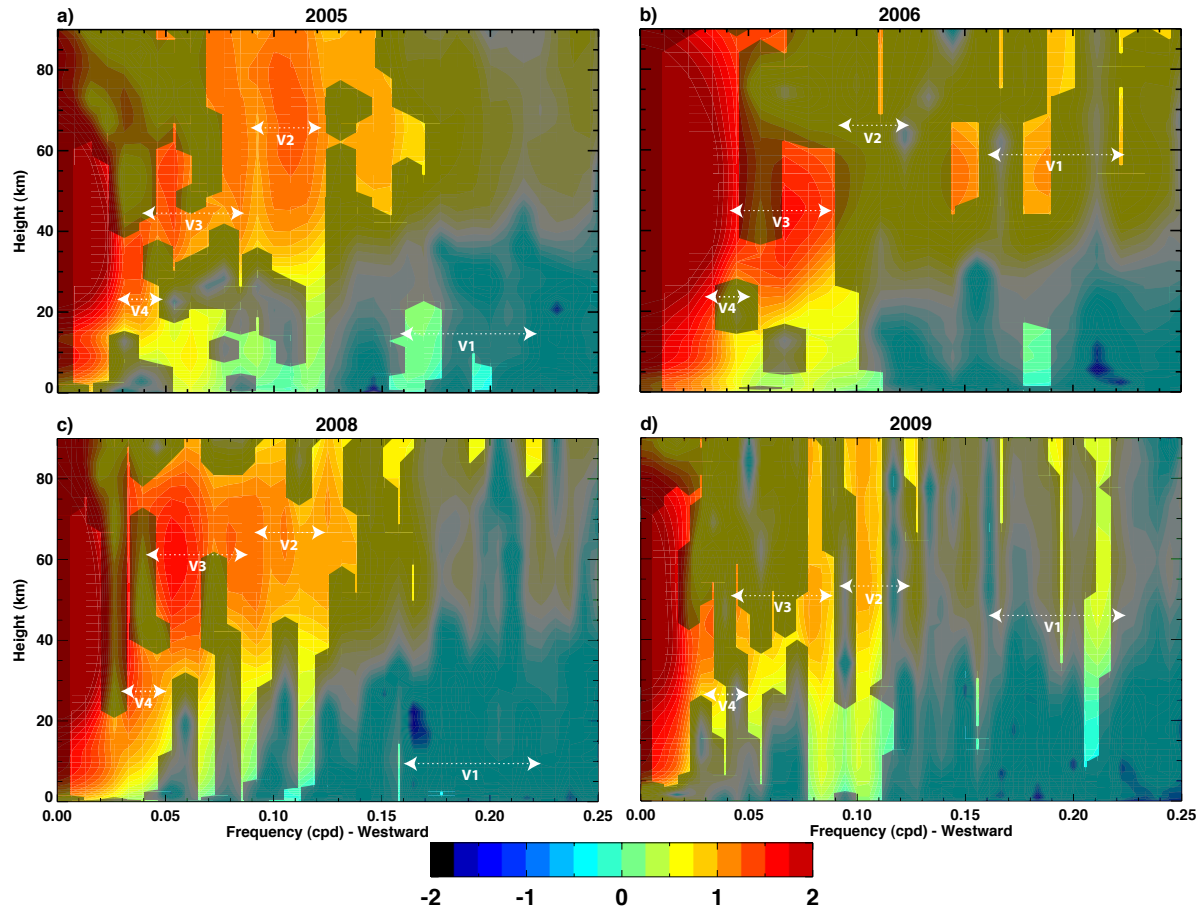


Figure 4. Amplitude spectrum of the wave-1 westward propagating modes as a function of altitude at 60 N. (a) 2005; (b) 2006; (c) 2008; (d) 2009. Color table is shown at the bottom as the \log_{10} of the amplitude in meters. Grey-ed out areas are not statistically significant based on the application of the band a priori hypothesis.

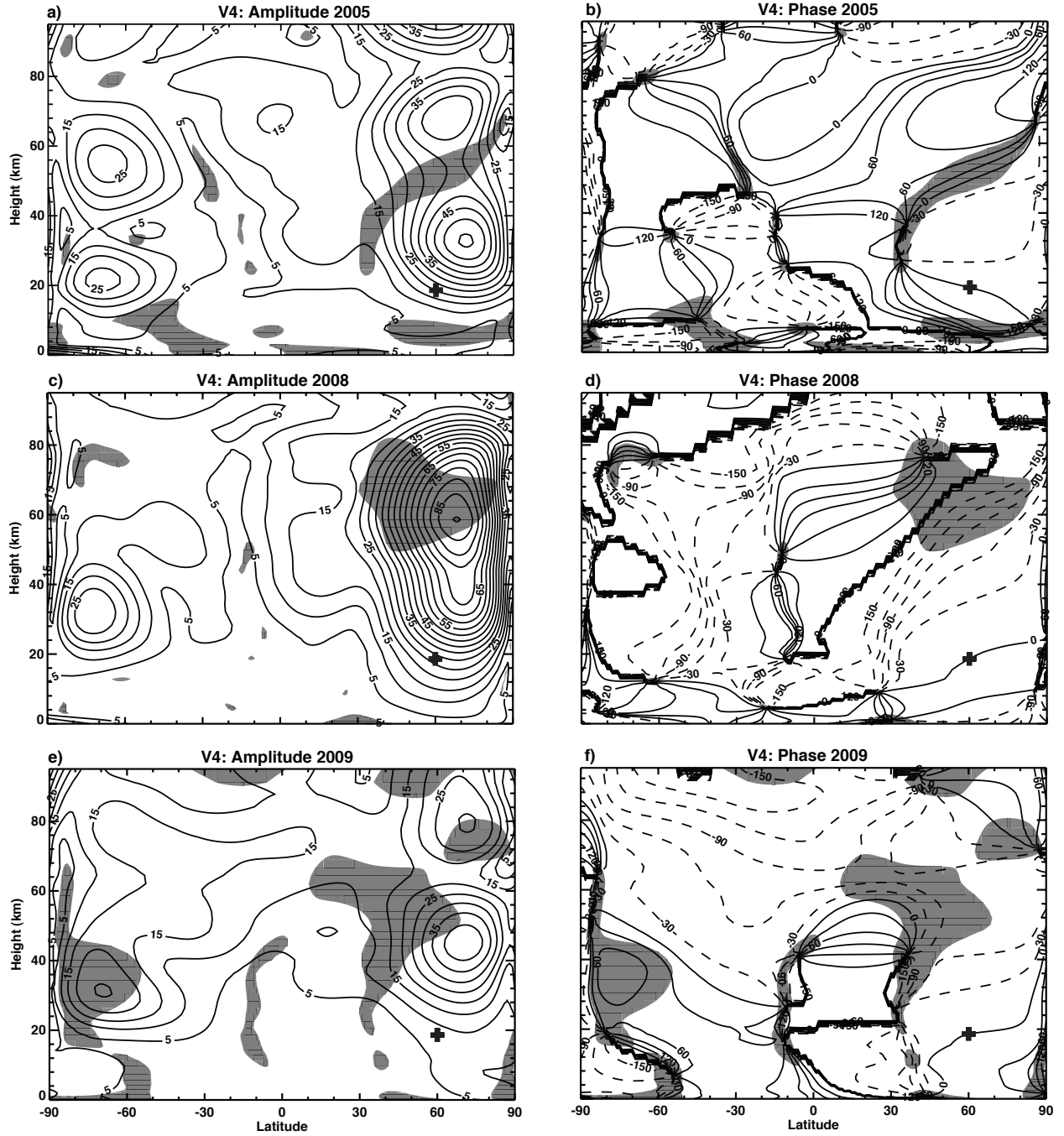


Figure 5. Amplitude and phase obtained from the coherence analysis of the V4 bands in Fig. 4. (a)-(b) are for 2005; (c)-(d) for 2008; (e)-(f) 2009. Unshaded areas have coherence above 0.9 with a reference point at 60N and 18 km. Contour interval is 5 m for the amplitude and 30° for the phase.

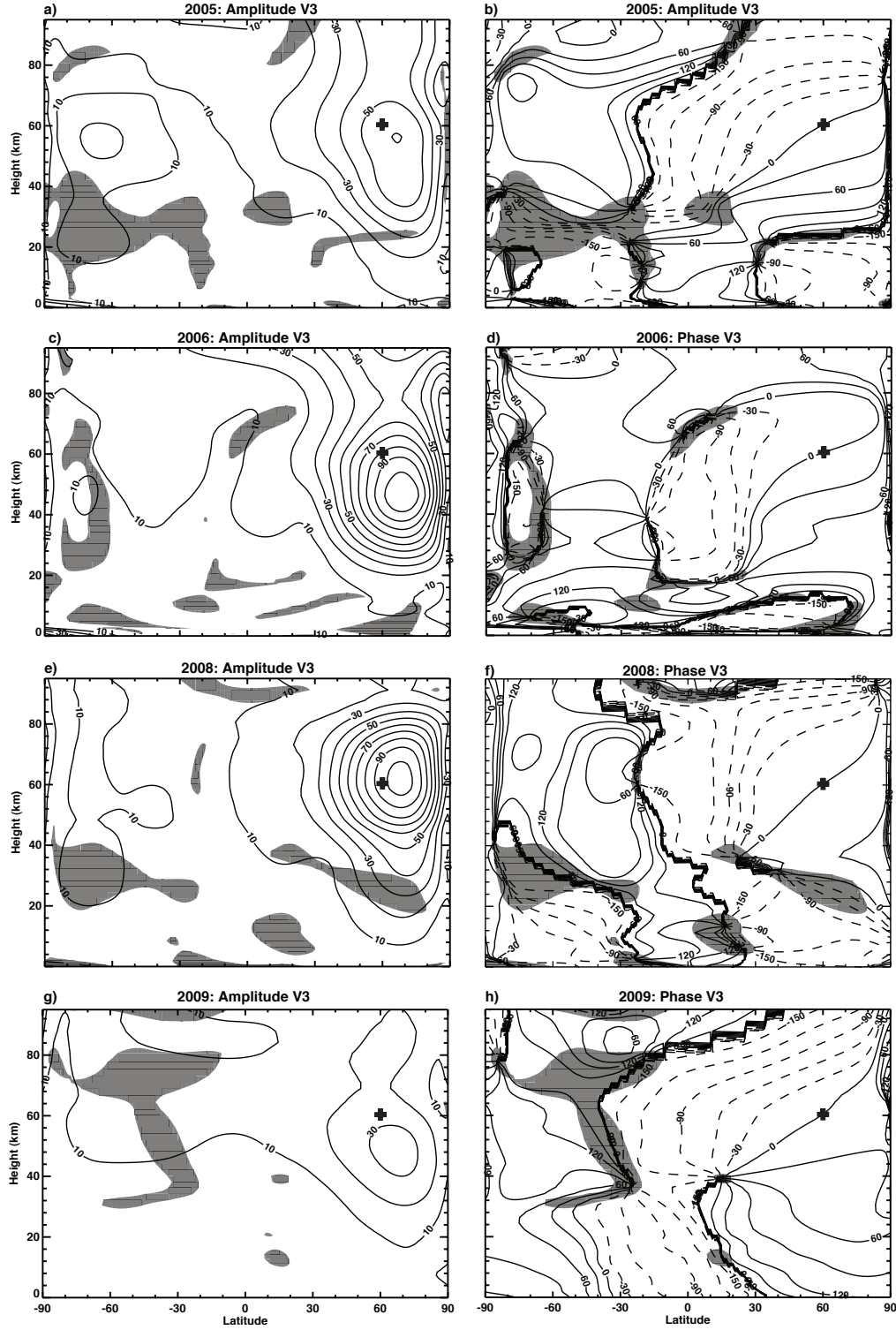


Figure 6. As in Fig. 5 but for the V3 band. (a) 2005, (b) 2006, (c) 2008, and (d) 2009. Contour interval is 10 m for the amplitude. Reference point is at 60°N and 60 km, indicated by the black cross.

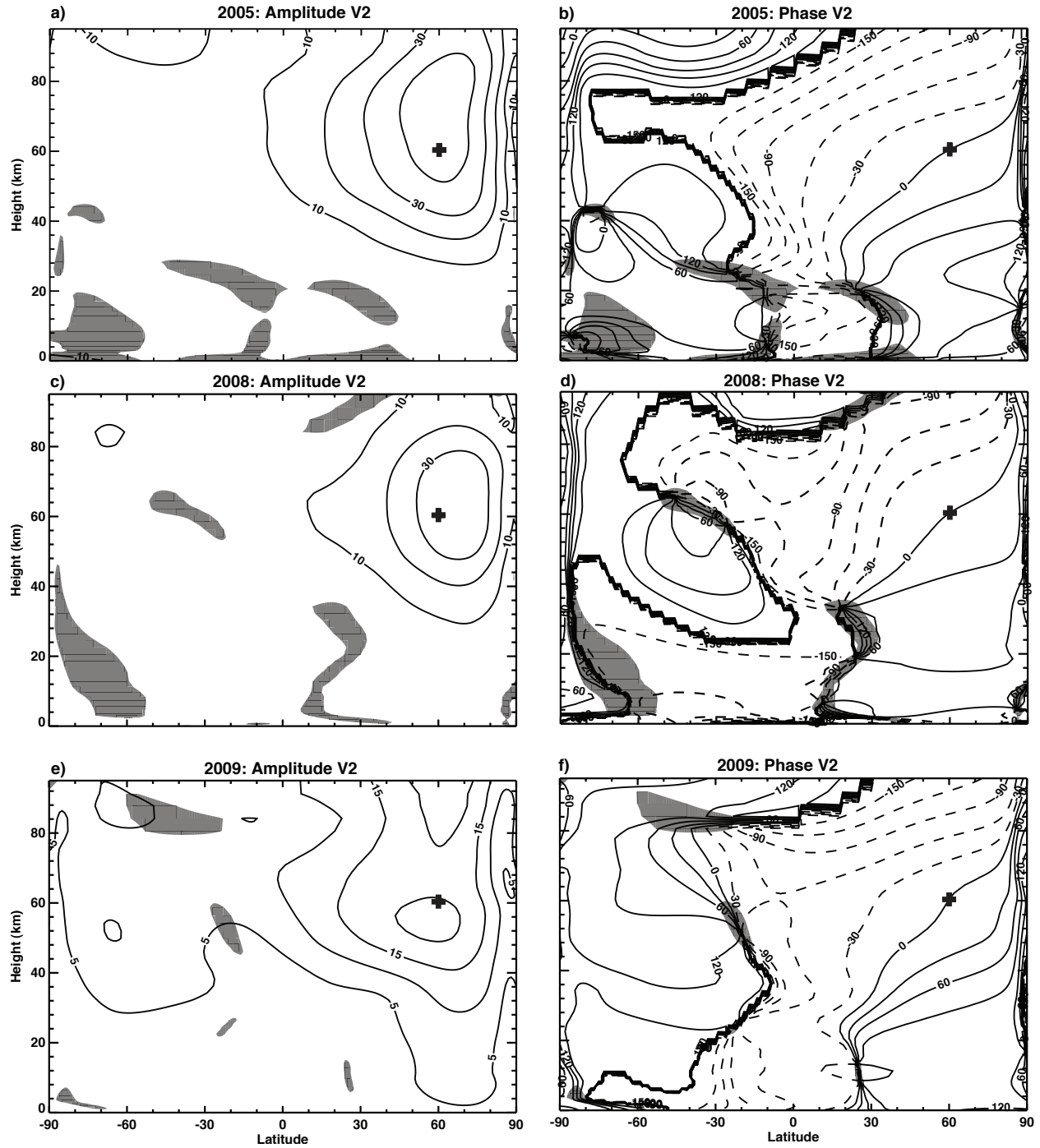


Figure 7. As in Fig. 5 but for the V2 bands. (a)-(b) 2005; (c)-(d) 2008; (e)-(f) 2009. Contour interval is 10 m for the amplitude in panels (a) and (c), and 5 m in panel (e). Contour interval for the phase 30° throughout. Reference point is at 60 N and 60 km, indicated by the black cross.

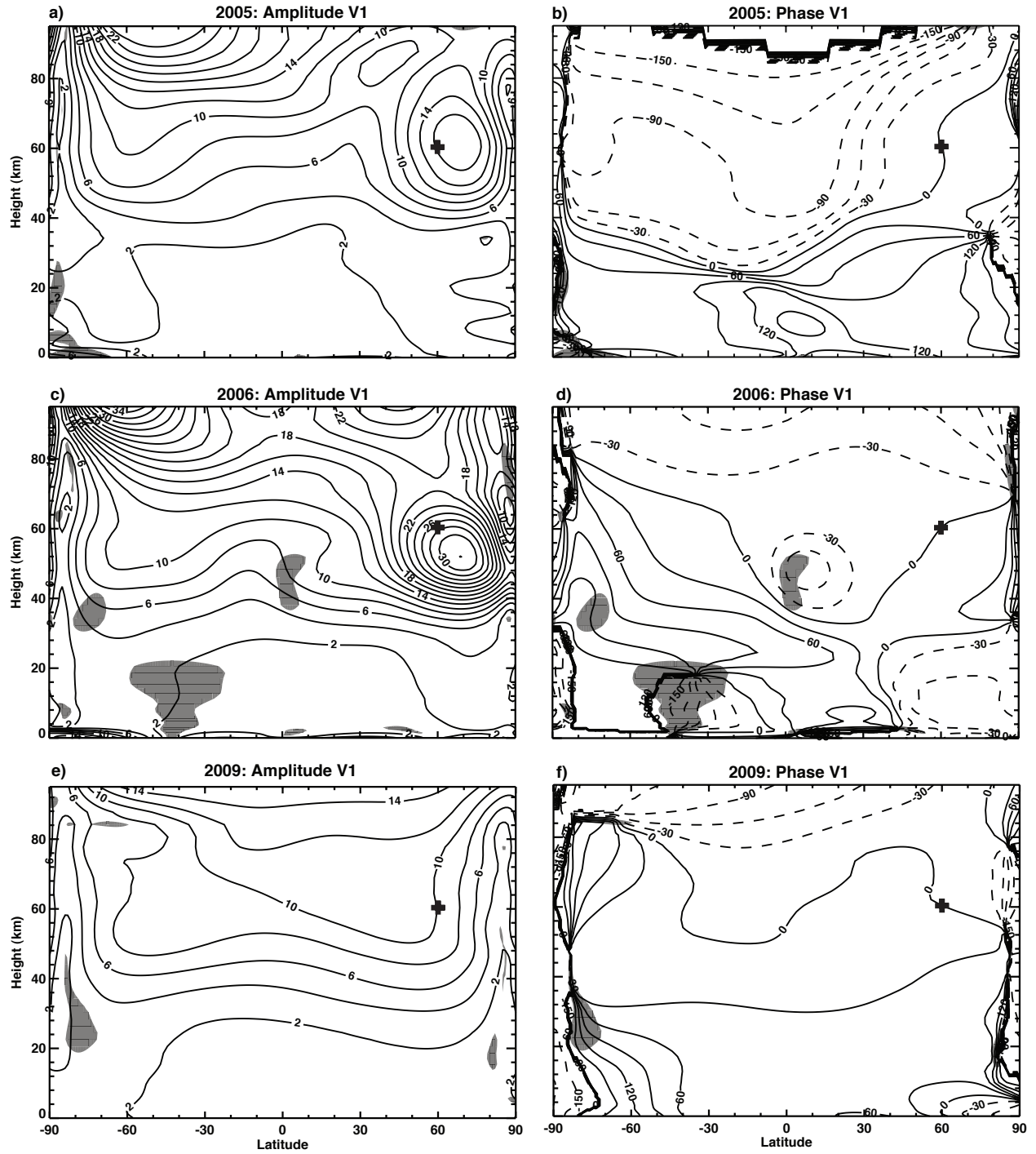


Figure 8. As in Fig. 5 but for the V1 band. (a-b) 2005, (c-d) 2006; (e-f) 2009. Contour interval for the amplitude plots is 2 m. Contour interval for the phase 30° throughout. Reference point is at 60°N and 60 km, indicated by the black cross.

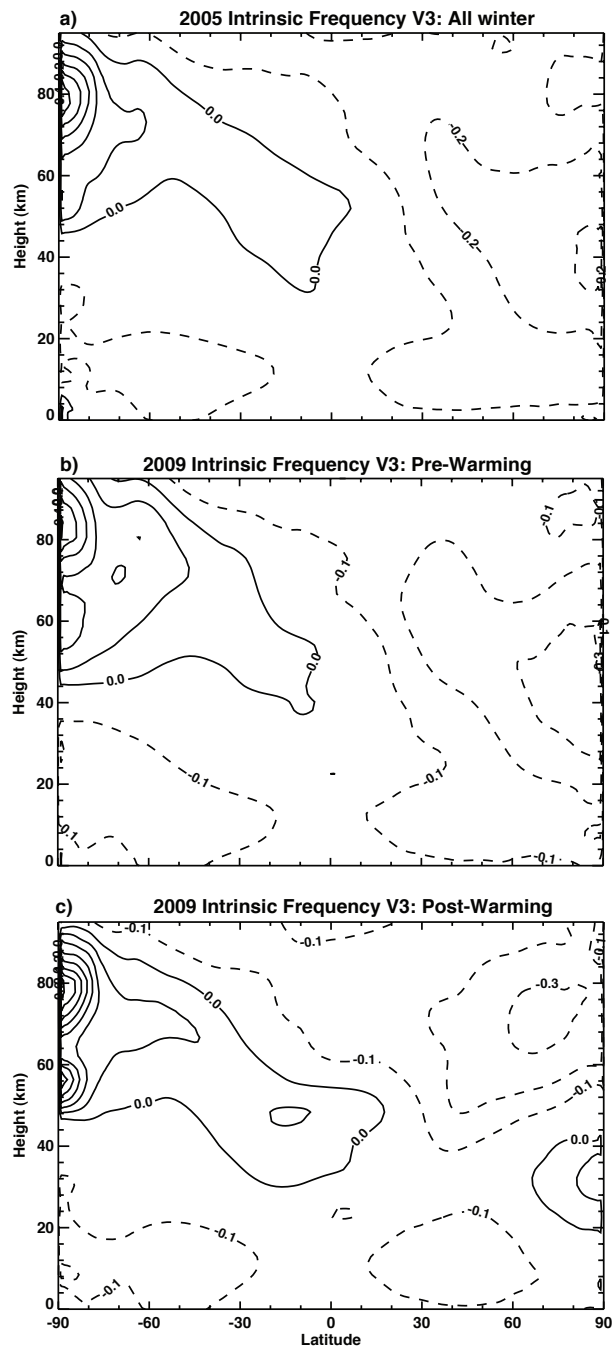


Figure 9. Intrinsic frequency (cpd) for the V3 band (a) during the entire winter of 2005; (b) in 2009 up to the day prior the SSW; (c) in 2009 from the day of the SSW through February 15 2009. Contour interval is 0.1 cpd.

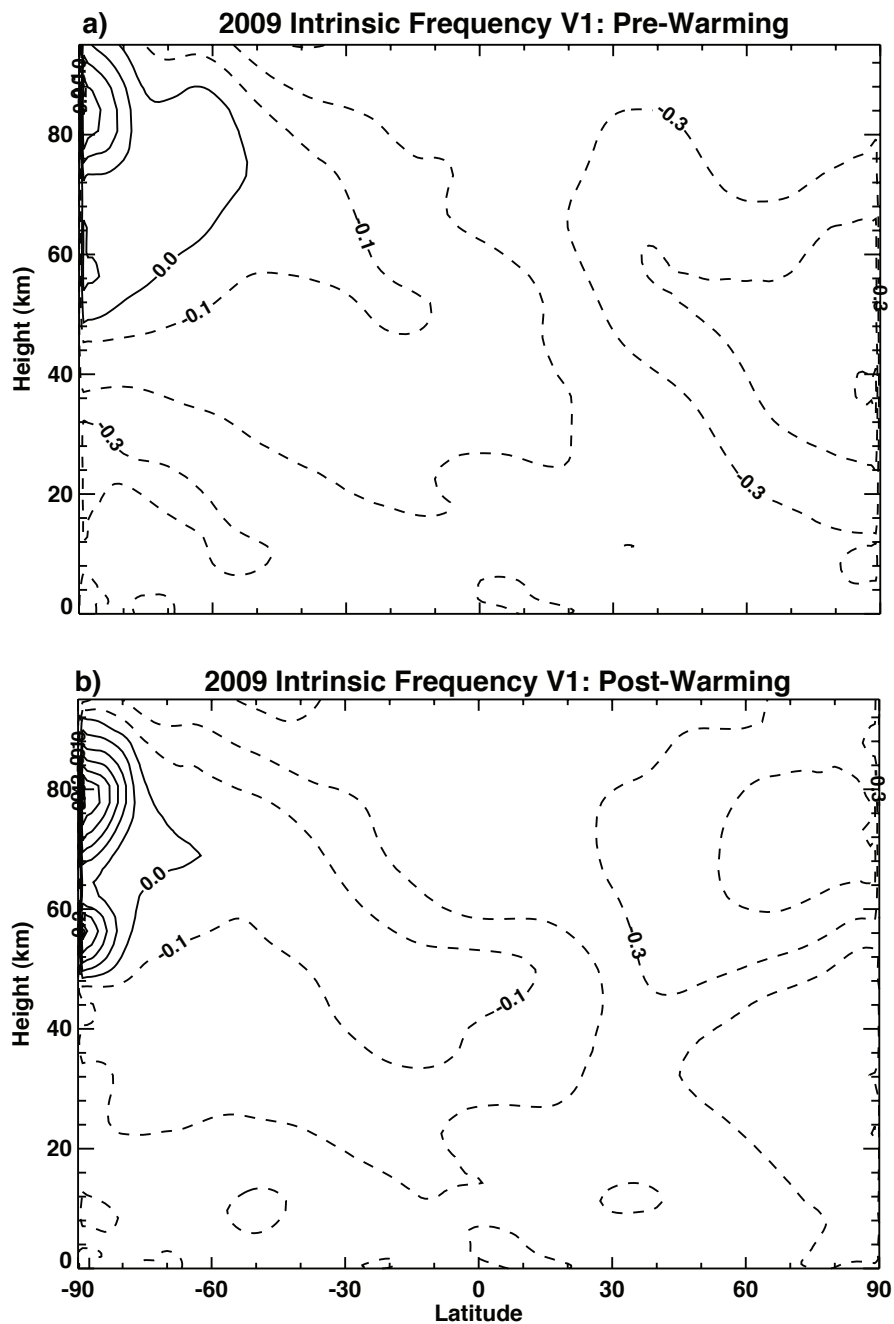


Figure 10. Intrinsic frequency (cpd) for the V1 band during the winter of 2009, (a) for days up to the day prior the SSW; (b) for days from the SSW to February 15 2009. Contour interval is 0.1 cpd.

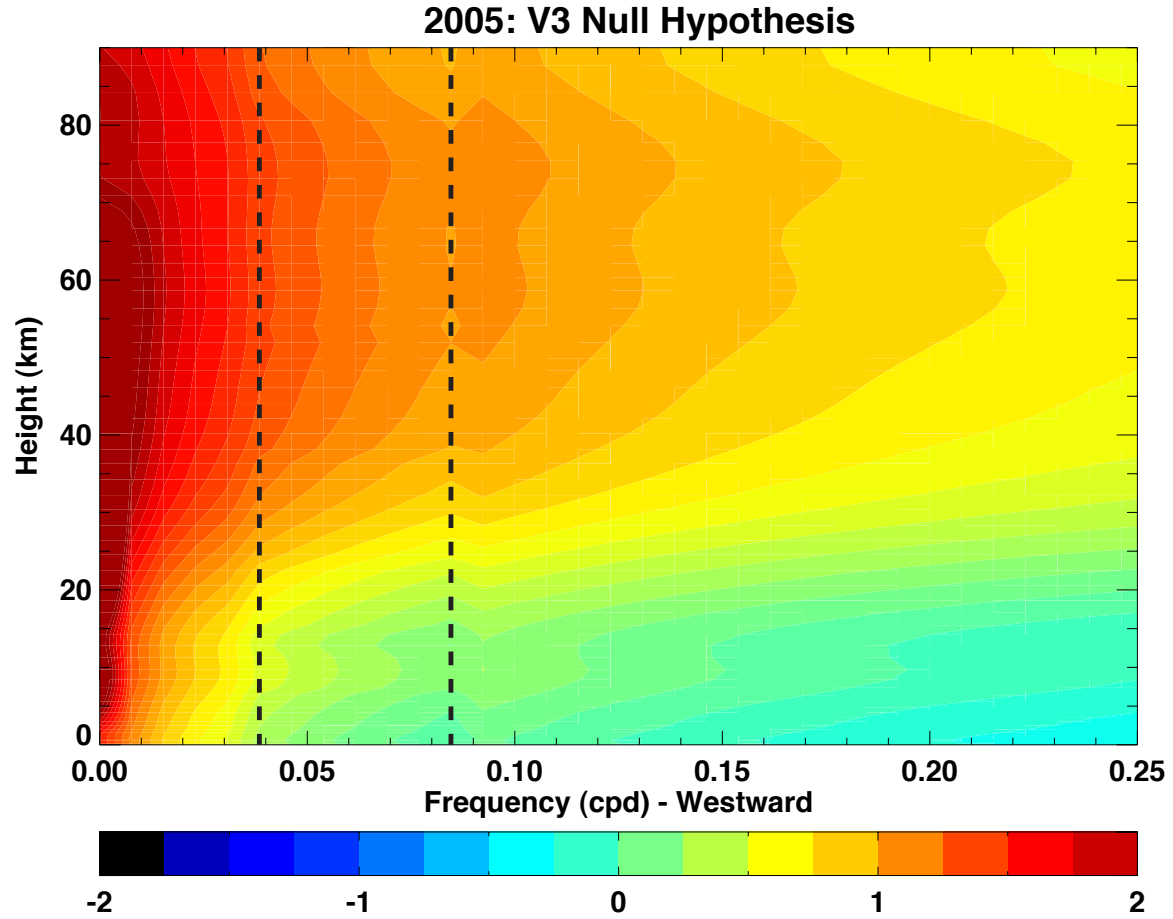


Figure A1. Amplitude of the null hypothesis obtained from the AR1 spectrum at wavenumber-1 and 60 N during the winter of 2005, using a 90% confidence interval. A *band a priori* hypothesis is used in the spectral range V3 (vertical black lines), but a *no a priori* hypothesis is used outside that range. The color bar at the bottom shows the \log_{10} of the amplitude.